Defects in AlSb: A density functional study

Mao-Hua Du
Materials Science and Technology Division and Center for Radiation Detection Materials and Systems, Oak Ridge National Laboratory, Oak Ridge, Tennessee 37831, USA
(Received 12 August 2008; revised manuscript received 29 December 2008; published 22 January 2009)

We carry out density functional calculations to study both intrinsic and extrinsic defects in AlSb. We focus on the carrier compensation and trapping properties of these defects, which are important to the radiation detection applications. We show that the Sb antisite (Sb_{Al}) is a low-energy defect, with interesting property of light-induced metastability, similar to the As antisite in GaAs. Sb_{Al} is effective in compensating holes induced by the residual carbon but is also a deep electron trap that reduces the carrier drifting length. We discuss the possibility of using hydrogenated isovalent N impurity in AlSb and GaAs to pin the Fermi level without causing efficient carrier trapping.

DOI: 10.1103/PhysRevB.79.045207 PACS number(s): 61.72.Bb, 61.72.J−, 71.55.Eq

I. INTRODUCTION

AlSb has potential applications in radiation detection for its relatively large band gap of 1.60 eV, which allows room-temperature applications, and high atomic number of Sb, which is necessary for sufficient stopping power of high-energy x and γ rays.[1,2] In semiconductor radiation detectors, the radiation-generated carriers are driven by the applied electric field and collected by the electrodes. Thus, high resistivity of the semiconductor material is needed to reduce the noise from the background free carriers and high $\mu\tau$ (μ is the carrier mobility and τ is the carrier lifetime) is required to enable carriers to drift to the electrodes. It has been found that the growth of single-crystal AlSb with high resistivity and high mobility is difficult.[1] AlSb is known to react with oxygen and almost all crucible materials. In addition, the volatility of Sb causes the nonstoichiometry of the material. All these problems are detrimental to the quality of the AlSb crystals. Both resistivity and mobility of AlSb currently fall behind those of CdZnTe,[1] another important radiation detection material.

Since purifying compound semiconductors to semi-insulating limit is not practical, carrier compensation is the primary way of achieving high resistivity of the material. Shallow dopants may be introduced for carrier compensation. For instance, the resistivity of the as-grown *p*-type AlSb can be increased by doping with Se and Te.[3] However, it is not possible to control the shallow dopant concentration to achieve the complete compensation of carriers. Thus, the pinning of Fermi level near the middle of the band gap is usually made possible by the existence of deep levels induced by defect or dopant.[4–6] Unfortunately, the deep levels are also efficient carrier traps and recombination centers, which reduce the carrier drifting length. Therefore, the understanding of the defect formation and the carrier trapping at defects is very important. First-principles calculations have identified low-energy intrinsic defects in AlSb.[7] In addition, unintentional dopants such as carbon and oxygen have been shown to affect the Fermi level significantly.[2,8] Carbon is a commonly found acceptor in AlSb, giving rise to *p*-type conductivity to the as-grown AlSb samples.[8] Oxygen increases the resistivity, but it also decreases the carrier mobility in AlSb significantly, which is detrimental to the detector performance.[2] Recent theoretical study on CdTe suggests that a complex of isovalent impurity and hydrogen, which is an amphoteric defect, may be effective in compensating either electron or hole carrier, which ever is in excess.[6]

In light of these recent developments, we carried out density functional calculations to study the intrinsic defects and impurities, including carbon, oxygen, sulfur, and silicon, in AlSb. We have also studied the possibility of introducing amphoteric N-H complex into AlSb and GaAs for carrier compensation purpose.

II. METHODS

A. Computational details

We performed calculations based on density functional theory with the Perdew-Burke-Ernzerhof generalized gradient correction,[9] as implemented in VASP.[10] The electron-ion interactions are described by projector augmented wave pseudopotentials.[11] The valence wave functions are expanded in a plane-wave basis with a cutoff energy of 400 eV. All the calculations were preformed using 64-atom cubic cells. A $2\times2\times2$ grid (with its origin shifted away from the Γ point) was used for the *k*-point sampling of Brillouin zone. All the atoms were relaxed to minimize the Feynman-Hellmann forces to below 0.02 eV/Å. The calculated AlSb lattice constant is 6.236 Å, in good agreement with the experimental values of 6.1355 Å.[12] For any charged defect, a jellium background of opposite charge is used to neutralize the supercell.

B. Defect formation energies and transition levels

The defect formation energy is given by

$$\Delta H_f = \Delta E - \sum_i n_i(\mu_i + \mu_i^{\mathrm{ref}}) + q(\varepsilon_{\mathrm{VBM}} + \varepsilon_f), \qquad (1)$$

where ΔE is the energy difference between the defect-containing and defect-free supercells and n_i is the difference in the number of atoms for the *i*th atomic species between the defect-containing and defect-free supercells. μ_i is a relative chemical potential for the *i*th atomic species referenced

 ©2009 The American Physical Society

to μ_i^{ref}. For Al and Sb, $\mu_{\text{Al}}^{\text{ref}}$ and $\mu_{\text{Sb}}^{\text{ref}}$ are the chemical potentials in bulk Al and bulk Sb, respectively. q in Eq. (1) is the defect charge state. If the system is under thermal equilibrium and there is no Al or Sb precipitation, we have $\mu_{\text{Al}} + \mu_{\text{Sb}} = \Delta H_f(\text{AlSb})$ and $\Delta H_f(\text{AlSb}) < \mu_{\text{Sb}} < 0$, where $\Delta H_f(\text{AlSb})$ is the heat of formation for AlSb. $\Delta H_f(\text{AlSb})$ is calculated to be −0.34 eV. ε_f in Eq. (1) is the Fermi energy referenced to the valance-band maximum (VBM) ε_{VBM}, which is taken as bulk VBM corrected by aligning the core potential of an atom (averaged within a sphere centered at the atom) far away from the defect in the defect-containing supercell with that in the defect-free supercell.[13] The defect transition energy level $\varepsilon(q/q')$ is the Fermi level ε_f in Eq. (1), at which the formation energies of the defect at the charge states q and q' are equal to each other.

AlSb has the zinc-blende structure and an indirect band gap of 1.60 eV.[12] The calculated indirect band gap is 1.21 eV. Note that the defect formation energy and the transition level are both determined by using the total energies calculated at special k points. Thus, for consistency, the energies of the VBM and the conduction-band minimum (CBM) for bulk AlSb were taken as averages over all special k points. This approach has been described in details in Ref. 13 and has been applied to many previous studies of defects in different systems.[6,14–17,19] There is only one nonequivalent k point in the $2\times2\times2$ k mesh for a perfect zinc-blende structure in a 64-atom cubic supercell. At the special k point, the VBM and CBM are down and up shifted by 0.18 and 0.12 eV, respectively, leading to the band gap of 1.51 eV. Although the band gap at the special k point is close to the experimental value, the arbitrary shift of the VBM and CBM causes uncertainty in the calculated deep level positions. However, the conclusions of this paper are not sensitive to the error related to the incorrect band gap.

C. Convergence tests

We have tested the convergence of the calculated defect formation energies with respect to the k mesh (up to a $4\times4\times4$ k mesh) and supercell size (up to a 216-atom supercell). The tests on the k mesh show that the calculated formation energies converge to within 0.1 eV. Regarding the finite supercell effect, we find that the formation energies for the neutral defects are also converged to within 0.1 eV. For charged defects, the errors are somewhat larger due to the electrostatic interaction between the charged defects and their periodic images. However, we do not apply any corrections to address such electrostatic interactions because the frequently used Makov-Payne correction[18] often significantly overestimates the correction.[19] We find that, by increasing the supercell to 216-atom cell using the equivalent k points, the formation energies of the Sb antisite at +2 charge state and the Al vacancy at −3 charge state increase by 0.08 and 0.20 eV, respectively. These errors include both the electrostatic and the strain effects arising from the finite supercell and should decrease if the defect charge is reduced.

III. RESULTS

A. Intrinsic defects

We have calculated formation energies for intrinsic point defects in AlSb, including vacancies, interstitial, split interstitials, and antisites. Figure 1 shows the calculated formation energies of several low-energy intrinsic defects in AlSb at both Al- and Sb-rich limits using Eq. (1). The growth condition for AlSb is usually Al rich.[2] If the AlSb sample undergoes postgrowth annealing under Sb overpressure, Sb-rich condition may also be accessed. Due to the unintentional carbon doping, the AlSb sample commonly exhibits p-type conductivity.[8] In p-type AlSb, it is evident from Fig. 1 that Al interstitial (Al_i) and Sb antisite (Sb_{Al}) are most important intrinsic defects that deserve careful studies.

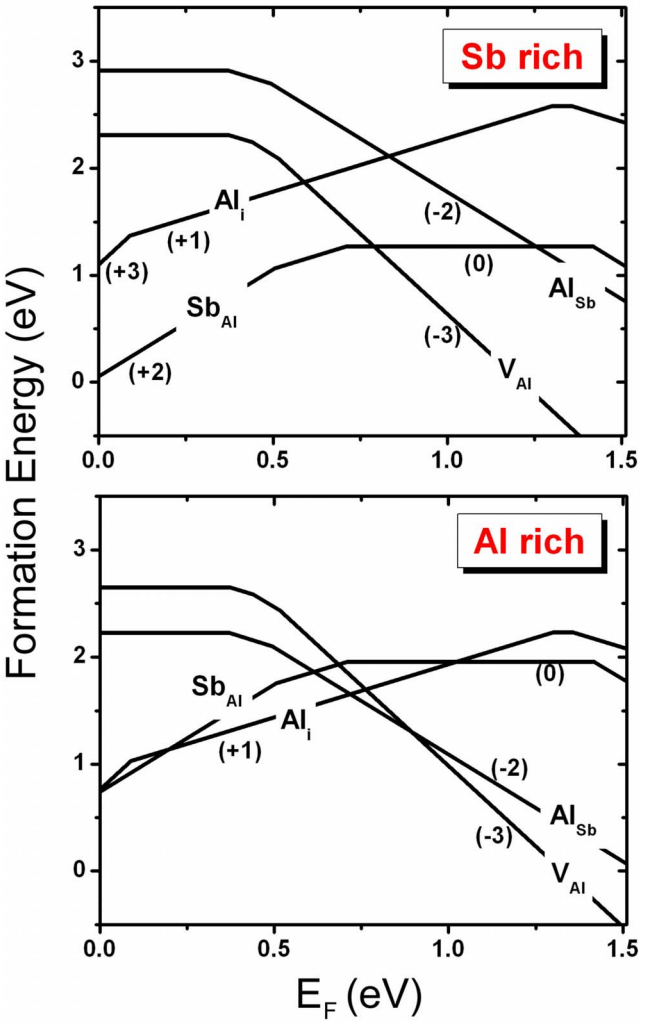

FIG. 1. (Color online) Calculated formation energies for low-energy intrinsic defects in AlSb as a function of electron Fermi energy at Sb-rich (top) and Al-rich (bottom) limits. The slope of an energy line indicates the charge state of the defect, as selectively shown. The transition levels are given by the Fermi energy at which the slope changes.

There are two Al_i sites. One is surrounded by four Al atoms (Al_i^{Al}) and the other is surrounded by four Sb atoms (Al_i^{Sb}). Al_i^{Al} is more stable than Al_i^{Sb} in all the relevant charge states except in +3 charge state. At the high ionization state of +3, Al_i^{+3} has large Coulomb attraction to the Sb anions and thus prefers the Al_i^{Sb} site. The singly positive charge state is the most stable charge state for Al_i over a large range of Fermi level, as shown in Fig. 1. The calculated diffusion

barrier for Al_i^+ is 1.28 eV,[20] which is in general lower than those for substitutional defects. During the slow cooling of the sample, the defects are in nearly equilibrium with their environment and are gradually annealed out until reaching the "freeze-in" temperature, at which the thermal equilibrium can no longer be maintained due to the insufficient thermal energy for driving defect diffusion. The lower diffusion barrier of Al_i means that Al_i can be gradually annealed out until a lower freeze-in temperature than other substitutional defects such as Sb_{Al}. If we define the freeze-in temperature as the temperature at which the defect can hop once per second and assume an attempting frequency for hopping as about 10^{13} s^{-1}, the freeze-in temperature for Al_i is roughly 500 K. But for a substitutional defect with diffusion barrier typically at least 2 eV, the freeze-in temperature would be higher than 800 K. Under these conditions, the concentration of Al_i would be lower than that of Sb_{Al} even under the Al-rich conditions.

The semiconductor radiation detector is operated under electric field. The charged defects with low diffusion barriers may diffuse, driven by the electric field, toward the electrode, leading to the detrimental effect of inhomogeneous electric-field distribution. The 1.28 eV diffusion barrier for Al_i renders Al_i nearly immobile at room temperature, in contrast to Cd_i^{+2} in CdTe, which has only a small calculated diffusion barrier of 0.36 eV.[6] Thus Al_i may pose a lesser problem in AlSb detector in terms of material homogeneity compared to Cd_i^{+2} in CdTe detector.

As argued above, Sb_{Al} may be the dominant intrinsic defect in *p*-type AlSb. At Sb-rich limit, the Sb_{Al} concentration $[Sb_{Al}]$ should be on the order of 10^{16} cm^{-3} according to the calculations. In addition, Sb_{Al} inserts deep donor levels in the band gap, as shown in Fig. 1. In GaAs, the anion antisite As_{Ga} is also an important defect which induces deep level that pins the Fermi level at midgap, thereby resulting in semi-insulating GaAs. However, Sb_{Al} in AlSb does not seem to be as effective as As_{Ga} in GaAs in terms of increasing resistivity as suggested by the much lower achieved resistivity of AlSb (Ref. 2) than GaAs.[21] This is perhaps because of the large amount of residual carbon acceptor ($\sim 10^{16}$–10^{17} cm^{-3}) (Refs. 2 and 8) in AlSb which may outnumber Sb_{Al}. It should be interesting to study Sb_{Al} to understand its role in carrier compensation, but, as far as we know, there has not been a comprehensive experimental defect characterization for AlSb. Our theoretical results below will show that Sb_{Al} should exhibit interesting photoinduced metastability, bearing much similarity to the famous EL2 defect[22] (attributed to As_{Ga})[23,24] in GaAs, and thus may be easily identified experimentally.

The ground-state structure of the neutral Sb_{Al} has the T_d symmetry. There exists a metastable structure of C_{3v} symmetry $[Sb_{Al}(C_{3v})]$. Its energy is higher than the ground state structure $[Sb_{Al}(T_d)]$ by 0.29 eV. In $Sb_{Al}(C_{3v})$, the Sb_{Al} atom moves into a trigonally symmetric interstitial position, as shown in Fig. 2. The neutral $Sb_{Al}(T_d)$ has an occupied single-particle defect level (optical level) near the midgap. This level is a *s*-like state centered at $Sb_{Al}(T_d)$. The neutral $Sb_{Al}(C_{3v})$ has an occupied single-particle level slightly above the VBM. These properties are similar to As_{Ga} in GaAs.[24] A schematic figure (Fig. 2) is drawn to show the optical and

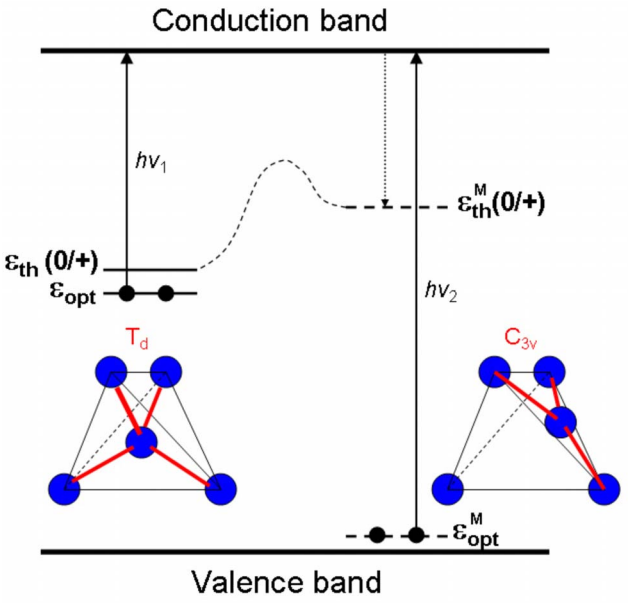

FIG. 2. (Color online) A schematic figure of the (0/+) thermodynamic transition levels and the single-particle defect levels for the ground-state (T_d) and the metastable (C_{3v}) neutral Sb_{Al} defect. The neutral $Sb_{Al}(T_d)$ has a fully occupied single-particle a_1 level, denoted as ε_{opt}, near the midgap. The electrons excited to the conduction band from the ε_{opt} level by photons of energy $h\nu_1$ can be thermally trapped (indicated by the dotted line) by the metastable-state defect thermodynamic transition level ε^M_{th} (0/+). The metastable structure is prohibited from relaxing to the ground state by a thermal barrier (indicated by the dashed curve) at low temperatures. The optical excitation ($h\nu_2$) can partially recover the ground-state structure from the metastable structure.

thermal ionization levels for $Sb_{Al}(T_d)$ and $Sb_{Al}(C_{3v})$. The metastability associated with the Sb antisite can cause the photoquenching of the optical absorption [associated with the ε_{opt} level of $Sb_{Al}(T_d)$ in Fig. 2] at low temperatures when exposed to subband gap light illumination ($h\nu_1$) because the photoexcited electron can be trapped by the ε^M_{th} level of $Sb_{Al}(C_{3v})$ driven by the coupling between the high-energy photoexcited electron and the lattice phonons. $Sb_{Al}(C_{3v})$ exhibits a large Stokes shift with its optical level insensitive to the photons with an energy of $h\nu_1$. The transformation from $Sb_{Al}(C_{3v})$ to $Sb_{Al}(T_d)$ is prohibited by the thermal barrier (calculated to be 0.23 eV)[20] at the low temperatures. The quenching of photocapacitance, photoluminescence, and the electron-paramagnetic resonance, which had been observed for the EL2 defect in GaAs (Ref. 22) due to the photoinduced metastability, may also be expected for Sb_{Al} in AlSb.

The ground-state $Sb_{Al}(T_d)$ can be recovered by thermal annealing at higher temperatures. At low temperatures (insufficient for thermal transformation to the ground-state structure), the continuous illumination by the near-band-gap photon source, $h\nu_2$ (see Fig. 2), should partially recover the ground-state $Sb_{Al}(T_d)$. Our calculations show that the photoionized $Sb_{Al}(C_{3v})^+$ and $Sb_{Al}(C_{3v})^{2+}$ can transform barrierlessly to their respective ground states, $Sb_{Al}(T_d)^+$ and $Sb_{Al}(T_d)^{2+}$, which can further absorb photoexcited electrons to become neutral $Sb_{Al}(T_d)$. However, the optical recovery of

$Sb_{Al}(T_d)$ may not be complete because Sb_{Al}^{+} and Sb_{Al}^{2+} can trap photoexcited electrons to become neutral $Sb_{Al}(C_{3v})$ again.

Figure 1 also shows a stable −2 charge state for Sb_{Al} with C_{1h} symmetry, similar to what Chadi[24] found for As_{Ga} in GaAs. The negatively charged anion site has also been found by calculations for Te_{Cd} in *n*-type CdTe.[25] Such anion antisite may be considered as a complex of cation vacancy and anion split interstitial (two anion atoms occupying one anion site). In *n*-type CdTe, V_{Cd} is −2 charged and $(Te\text{-}Te)_{spl}$ is neutral. Thus, their complex Te_{Cd} is −2 charged. In *n*-type AlSb, V_{Al} is −3 charged and $(Te\text{-}Te)_{spl}$ is −1 charged. Their complex Sb_{Al} is thus −4 charged. However, structural relaxation occurs. The interstitial Sb relaxes to break one Al-Sb bond and make two Sb-Sb bonds with the Sb atoms around the vacancy, thereby reducing the stable charge state to −2. We suggest that the structural model of a complex of cation vacancy and anion split interstitial may be generally applied to anion antisite in III-V and II-VI semiconductors and thus the anion antisite may be amphoteric in many of these semiconductors.

B. Extrinsic defects

Commonly encountered extrinsic defects in AlSb include C, O, Si, S, etc.[2] C_{Sb} is found to be much more stable than C_{Al}, in agreement with Lordi *et al.*[2] C_{Sb} is a shallow acceptor with calculated (0/−) transition level of $E_{VBM}+0.1$ eV. The hydrogenation of the C_{Sb} results in a C_{Sb}-H complex in C_{3v} symmetry, having a strong C-H bond with calculated stretching frequency of 2772 cm^{-1} and calculated doubly degenerate wagging frequency of 771 cm^{-1}.[26] The calculated stretching frequency is somewhat larger than the experimentally measured value[8] of 2566.6 cm^{-1}, which may be the result of the harmonic approximation used in the dynamic matrix approach that typically overestimates H stretching modes.

Oxygen can occupy Sb site (O_{Sb}) as an electron donor in *p*-type AlSb. When the Fermi level is raised, O_{Sb} favors a structural transformation to become an acceptor. As an acceptor, O_{Sb} is twofold coordinated with two Al-O_{Sb} bonds broken. The two Al atoms that break apart from O_{Sb} make a new Al-Al bond. This is essentially the so-called α-CCB-DX structure (CCB stands for cation-cation bond).[27,28] It is well known that shallow donors in semiconductors often exhibit DX transformations to become deep acceptors.[29] There is another DX structure, β-CCB-DX,[27,28] for O_{Sb}. The calculated formation energies of these two DX structures are nearly the same with difference within the numerical uncertainty. The interstitial and split interstitial O are also of low energy as shown in Fig. 3 for the Al-rich limit. Due to the amphoteric behavior of O, as shown in Fig. 3, a large amount of oxygen in AlSb can pin the Fermi level and increase the resistivity of AlSb as observed in Ref. 2. Note that, for the formation energies shown in Fig. 3, the O chemical potential satisfies the following relation that prevents the formation of Al_2O_3: $3\mu_O+2\mu_{Al}<\Delta H_f(Al_2O_3)$, where $\Delta H_f(Al_2O_3)$ is the heat of formation of Al_2O_3 calculated to be −14.13 eV. In reality, this relation may not be satisfied and thus the surface oxidation occurs. Due to the strong tendency to form oxide, O in AlSb may be easily annealed out to the surface to form oxide layer.

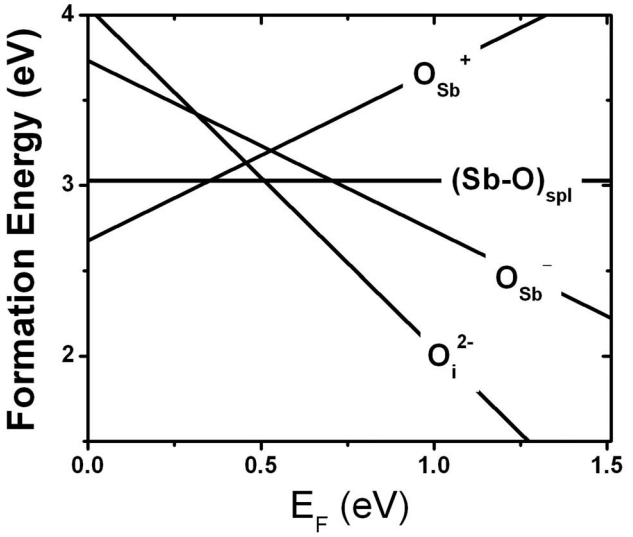

FIG. 3. Calculated formation energies for substitutional O (O_{Sb}), O split interstitial $(Sb\text{-}O)_{spl}$, and O interstitial (O_i) (centered at Al tetrahedron) in AlSb at Al-rich limit.

Similar to O_{Sb}, substitutional sulfur S_{Sb} can take α- and β-CCB-DX structures[27,28] with β-CCB-DX being more stable by only 0.03 eV according to our calculations. The (+/−) transition level between S_{Sb}^{+} and $S_{Sb,DX}^{-}$ is calculated to be $E_{VBM}+1.15$ eV. The DX center has been found experimentally in Se-doped *n*-type AlSb (Ref. 30) and may also exist in Te-doped AlSb. Si is also amphoteric in AlSb, either a donor Si_{Al}^{+} or an acceptor Si_{Sb}^{-}. The (+/−) transition level is calculated to be $E_{VBM}+0.62$ eV$+\mu_{Sb}$, where −0.34 eV $[\Delta H(AlSb)]<\mu_{Sb}<0$.

IV. DISCUSSIONS

A. Can Sb_{Al} improve the performance of AlSb detector?

We have identified deep donors (e.g., Sb_{Al}) and amphoteric defects (e.g., O_{Sb} and S_{Sb}) from the results shown above. The deep levels are desired for the purpose of Fermi-level pinning. The as-grown AlSb is typically *p* type due to the residual carbon impurities. It may be tempting to increase the Sb_{Al} concentration $[Sb_{Al}]$ to increase resistivity. However, the deep levels are also deep carrier traps, resulting in reduced carrier drifting length. The lesson may be learned from GaAs. GaAs has been studied as a radiation detector since 1960s. Both resistivity ($>10^7$ Ω cm) and carrier concentration ($<10^7$ cm^{-3}) approach theoretical intrinsic limit. The carrier compensation in high-resistivity GaAs is accomplished by the presence of defect donor level EL2 ($\sim 10^{16}$ cm^{-3}),[4] which has been assigned to As_{Ga}.[23,24] On the other hand, the GaAs detector is also plagued by these deep levels that can trap carriers efficiently and do not release them within the charge collection time. Thus, increasing $[Sb_{Al}]$ in AlSb may lead to the same dilemma for GaAs that is the irreconcilability between high resistivity and long car-

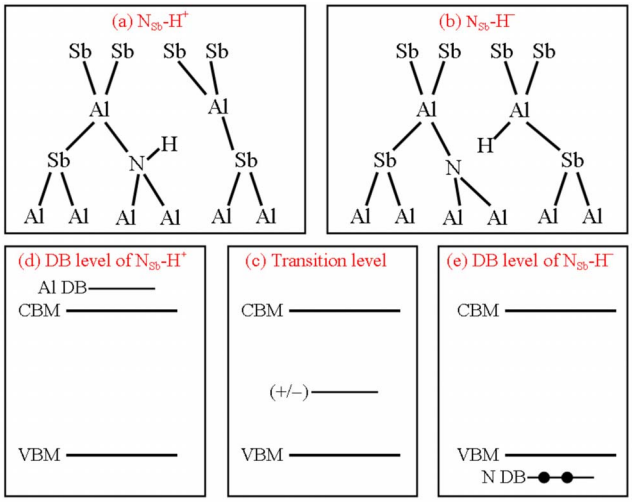

FIG. 4. (Color online) Schematic pictures of the structures, the thermodynamic transition level, and the single-particle dangling-bond (DB) levels of the N_{Sb}-H complex. The defect levels are shown with respect to the VBM and the CBM. (a) The structure of N_{Sb}-H^+, (b) the structure of N_{Sb}-H^-, (c) the thermodynamic transition level induced by N_{Sb}-H, (d) the single-particle Al DB level induced by N_{Sb}-H^+, and (e) the single-particle N DB level induced by N_{Sb}-H^-. The electron occupations on the single-particle are indicated by the black dots.

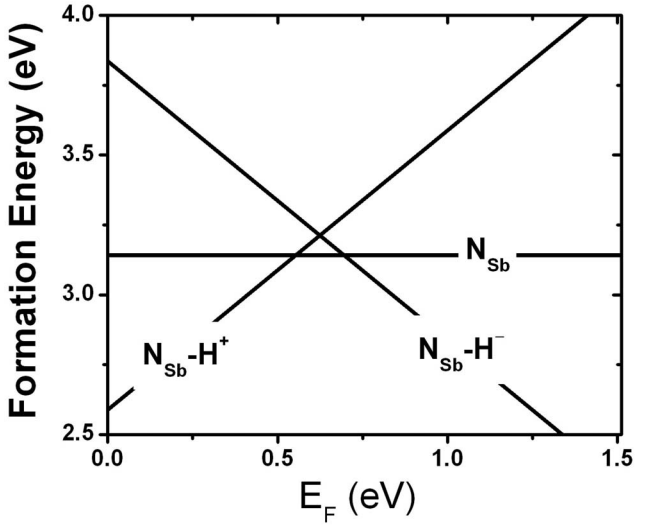

FIG. 5. Calculated formation energies for substitutional N (N_{Sb}) and hydrogenated N_{Sb} in AlSb when $\mu_H=0$. The structures of N_{Sb}-H^+ and N_{Sb}-H^- are shown schematically in Figs. 4(a) and 4(b), respectively.

rier drifting length. Figure 1 suggests that the Al-rich growth condition actually leads to lower defect concentrations especially in *p*-type AlSb. If $[Sb_{Al}]$ can be effectively reduced by changing the growth conditions, the carrier traps can be reduced, but the alternative carrier compensation method is needed.

B. N_{Sb}-H in AlSb

Recently we have suggested that the complex of isovalent impurity (on anion site) and hydrogen may be an effective carrier compensator because such defect introduces a (+/−) transition level near the midgap.[6] Typically, the isovalent impurity needs to be strongly H bound (such as N and O) to ensure a reasonable concentration of the hydrogenated impurity. It has been shown that O_{Te}-H in CdTe can pin the Fermi level near the midgap without causing electron trapping.[6] We apply this strategy here by considering the N_{Sb}-H complex in AlSb.

At +1 charge state of N_{Sb}-H, H binds N at the bond-center (BC) position [Fig. 4(a)]. At −1 charge state, H binds with Al at the BC position [Fig. 4(b)]. The (+/−) transition level is calculated to be $E_{VBM}+0.62$ eV. The neutral N_{Sb}-H is unstable. For N_{Sb}-H^+, the empty Al orbital on the threefold-coordinated Al resonates with the conduction band and thus does not trap electrons. For N_{Sb}-H^-, the fully occupied lone-pair orbital on the threefold-coordinated N_{Sb} resonates with the valence band and thus does not trap holes. Figures 4(c)–4(e) show schematically the thermodynamic transition level and the single-particle dangling-bond levels induced by the N_{Sb}-H complex. Based on these results, N_{Sb}-H may be an effective carrier compensator (while not being a deep trap) if it can exist in AlSb in relatively large quantity. However, the calculated formation energy for N_{Sb} is very high (see Fig. 5), which would give negligible N_{Sb} concentration. This is because the requirement of not forming second phase of AlN limits the upper bound of N chemical potential such that $\mu_N+\mu_{Al}<\Delta H_f(AlN)$, where $\Delta H_f(AlN)$ is the heat of formation of AlN calculated to be −2.85 eV (compared to the experimental value of −3.22 eV.[31]) If this restriction can be lifted, which means the growth of AlSb needs to tolerate the surface nitridation, the N_{Sb} concentration can be increased. However, any prolonged thermal annealing could drive substitutional N to the surface to form AlN.

C. N_{As}-H in GaAs

Since the N solid solubility in AlSb is very low, maybe GaAs should be revisited using N-H complex as a carrier compensator. As for the deep donor As_{Ga}, it can be removed by the heat treatment.[32] The heat of formation for GaN is calculated to be −1.74 eV (compared to the experimental value of −1.63 eV), which is much smaller than that for AlN.[31] This means that the nitride phase segregation poses a much smaller problem for N doping of GaAs than for N doping of AlSb. The calculated minimum formation energy for N_{As} in GaAs is 1.76 eV, which is much smaller than that for N_{Sb} (3.14 eV) in AlSb and can bring the N_{As} concentration in GaAs on the order of 10^{16} cm^{-3}. The calculated hydrogenation energy of N_{As} in GaAs is fairly low.[33] The hydrogen concentration was found to be about 1 order of magnitude lower than the nitrogen concentration in GaAsN alloy grown by metal organic chemical vapor epitaxy.[34] The (+/−) transition level for N_{As}-H in GaAs had been calculated to be $E_{VBM}+0.83$ eV near the midgap of GaAs.[33] (The band gap of GaAs is 1.42 eV.) Thus, N_{As}-H may be used as effective carrier compensator in GaAs.

Reference 33 shows that the H binds with N_{As} at the bond-center site for both N_{As}-H^+ and N_{As}-H^- in GaAs. The

structure of N_{As}-H^+ in GaAs is similar to the structure of N_{Sb}-H^+ in AlSb. N_{As}-H^+ does not induce a single-particle defect level inside the band gap. The Ga dangling-bond level in N_{Sb}-H^+ is resonant in the conduction band. Thus, N_{As}-H^+ is not effective in electron trapping in GaAs. However, the structure of N_{As}-H^- in GaAs is different from that of N_{Sb}-H^- in AlSb in that H binds with N rather than with the cation.[33] This leaves a fully occupied Ga dangling-bond level inside the band gap. Thus, N_{As}-H^- in GaAs is a hole trap, in contrast to N_{Sb}-H^- in AlSb, which does not induce any hole-trapping levels in the band gap. It had been shown previously that O_{Te}-H^- in CdTe is also a hole trap because H binds with O_{Te} (at the antibonding site), leaving an occupied Cd lone-pair level in the band gap.[6] Generally, the hydrogenated isovalent impurity is not an electron trap, but it may or may not be a hole trap depending on the H binding site.

D. Isolated-N-induced defect levels in GaAs and AlSb

The use of the complex of isovalent impurity and hydrogen for carrier compensation inevitably also brings a large amount of unhydrogenated isovalent impurities into the host semiconductor. An isovalent impurity with electronegativity much larger than the host atom generally introduces an empty a_1 level near the CBM, which could be either resonant state or trap state depending on the host materials.[35] When the concentration of the isovalent impurity increases to alloy limit ($\sim$1 at. %), the strong coupling between the isovalent impurity level and the CBM state causes anticrossing of the two levels[36,37] and can lower the band gap significantly as manifested by N in GaAs.[38] However, for the nitrogen concentration considered here ($\sim 10^{16}$ cm^{-3}), the perturbation of the CBM state by N is small and should not cause significant scattering of the electron carriers in the CBM state. The isolated N in GaAs is also not an electron trap because its level is at $E_{CBM}+0.18$ eV.[39] However, it is not clear about the N level position in AlSb. The small-supercell calculation actually represents the alloy situation, in which a deep band with large N character appears inside the AlSb band gap (or a new lower band edge is formed in AlSbN alloy). Therefore, one cannot obtain the isolated N level in small-supercell calculations. It was found that at least several thousand atoms are needed in a supercell approach to get relatively converged result for isolated isovalent impurity levels.[35,40] It is often assumed that a localized defect level approximately lines up in absolute energy scale in different semiconductors. Using the calculated valence-band offset between GaAs and AlSb (0.15 eV) (Ref. 41) and the experimental band gaps of these two semiconductors (1.42 and 1.60 eV, respectively), one can find that the N impurity level in GaAs lies about 0.15 eV below the CBM of AlSb in absolute scale. Since the Al-N bond is stronger than the Ga-N bond, the N level in AlSb should be shifted up somewhat (perhaps a few tenths of eV) relative to that in GaAs because of the antibonding nature of this level.[35] But since we are unable to carry out large-supercell calculations with thousands of atoms, we cannot pin down the level position for isolated N in AlSb. We can only conclude that the N level is near the CBM of AlSb and is likely to be in the conduction band.

In the small-supercell calculations, the isovalent impurity hydrogenated with one hydrogen atom still induces a deep empty gap state which is a little higher ($\sim$0.1 eV) than that for unhydrogenated isovalent impurity. Based on the discussions above, this level is expected to move up into the conduction band in a converged large-supercell calculation.

V. CONCLUSIONS

We have studies the defects in AlSb to understand their effects on resistivity and carrier trapping, which are important for radiation detection applications. We show that Sb_{Al} should be an important intrinsic defect in AlSb, which not only has low formation energy but also induces deep donor levels in the band gap which may play an important role in carrier compensation. Our results also suggest that Sb_{Al} may have the photoinduced metastability similar to As_{Ga} in GaAs. The substitutional oxygen has a stable DX structure, giving rise to a deep carrier-trapping level that may pin the Fermi level. However, all these deep levels pose serious problem on the carrier drifting length and this problem may not be easily circumvented, which is the case for GaAs. In light of this, we suggest that a complex of isovalent impurity and hydrogen may provide a carrier compensation mechanism for both electrons and holes without causing significant carrier trapping at least for electrons. Our calculations show that the substitutional N in GaAs can have a sufficiently high concentration. Thus, we suggest further experimental study on the carrier compensating property of N_{As}-H in GaAs. However, the N_{Sb} or N_{Sb}-H concentration in AlSb is predicted to be too low to have a significant impact on the resistivity of the material.

ACKNOWLEDGMENTS

The author is grateful for helpful discussions with D. J. Singh. This work was supported by the U.S. DOE Office of Nonproliferation Research and Development NA22.

[1] V. E. Kutny, A. V. Rybka, A. S. Abyzov, L. N. Davydov, V. K. Komar, M. S. Rowland, and C. F. Smith, Nucl. Instrum. Methods Phys. Res. A **458**, 448 (2001).

[2] V. Lordi, D. Aberg, P. Erhart, and K. J. Wu, Proc. SPIE **6706**, 67060O (2007).

[3] A. Herczog, R. R. Haberecht, and A. E. Middleton, J. Electrochem. Soc. **105**, 533 (1958).

[4] G. M. Martin, J. P. Farges, G. Jacob, J. P. Hallais, and G. Poiblaud, J. Appl. Phys. **51**, 2840 (1980).

[5] M. Fiederle, C. Eiche, M. Salk, R. Schwarz, K. W. Benz, W. Stadler, D. M. Hofmann, and B. K. Meyer, J. Appl. Phys. **84**, 6689 (1998).

[6] M.-H. Du, H. Takenaka, and D. J. Singh, Phys. Rev. B **77**, 094122 (2008).
[7] D. Aberg, P. Erhart, A. J. Williamson, and V. Lordi, Phys. Rev. B **77**, 165206 (2008).
[8] M. D. McCluskey, E. E. Haller, and P. Becla, Phys. Rev. B **65**, 045201 (2001).
[9] J. P. Perdew, K. Burke, and M. Ernzerhof, Phys. Rev. Lett. **77**, 3865 (1996).
[10] G. Kresse and J. Furthmüller, Phys. Rev. B **54**, 11169 (1996).
[11] G. Kresse and D. Joubert, Phys. Rev. B **59**, 1758 (1999).
[12] *CRC Handbook of Chemistry and Physics*, 88th ed., edited by D. R. Lide (CRC/Taylor and Francis, Boca Raton, FL, 2008).
[13] S. B. Zhang, J. Phys.: Condens. Matter **14**, R881 (2002).
[14] A. Janotti, S.-H. Wei, and S. B. Zhang, Appl. Phys. Lett. **83**, 3522 (2003).
[15] S. Limpijumnong, S. B. Zhang, S.-H. Wei, and C. H. Park, Phys. Rev. Lett. **92**, 155504 (2004).
[16] C. G. Van de Walle, S. Limpijumnong, and J. Neugebauer, Phys. Rev. B **63**, 245205 (2001).
[17] M.-H. Du, H. M. Branz, R. S. Crandall, and S. B. Zhang, Phys. Rev. Lett. **97**, 256602 (2006).
[18] G. Makov and M. C. Payne, Phys. Rev. B **51**, 4014 (1995).
[19] D. Segev and S.-H. Wei, Phys. Rev. Lett. **91**, 126406 (2003).
[20] The diffusion barriers are calculated using nudged elastic band method. The details of the method are given by G. Henkelman and H. Jónsson, J. Chem. Phys. **113**, 9978 (2000).
[21] S. P. Beaumont *et al.*, Nucl. Instrum. Methods Phys. Res. A **322**, 472 (1992).
[22] G. M. Martin and S. Makram-Ebeid, in *Deep Centers in Semiconductors*, edited by S. T. Pantelides (Gordon and Breach, New York, 1992).
[23] J. Dabrowski and M. Scheffler, Phys. Rev. Lett. **60**, 2183 (1988).
[24] D. J. Chadi, Phys. Rev. B **68**, 193204 (2003).
[25] M.-H. Du, H. Takenaka, and D. J. Singh, J. Appl. Phys. **104**, 093521 (2008).
[26] The hydrogen local vibrational frequencies are calculated by diagonalization of the dynamical matrix (mass-weighted Hessian matrix), which is built by the second derivatives of the total energy with respect to the atomic positions.
[27] M.-H. Du and S. B. Zhang, Phys. Rev. B **72**, 075210 (2005).
[28] M.-H. Du, Appl. Phys. Lett. **92**, 181908 (2008).
[29] P. M. Mooney, J. Appl. Phys. **67**, R1 (1990).
[30] P. Becla, A. Witt, J. Lagowski, and W. Walukiewicz, Appl. Phys. Lett. **67**, 395 (1995).
[31] M. R. Ranade, F. Tessier, A. Navrostsky, and R. Marchand, J. Mater. Res. **16**, 2824 (2001).
[32] J. Lagowski, H. C. Gatos, C. H. Kang, M. Skowronski, K. Y. Ko, and D. G. Lin, Appl. Phys. Lett. **49**, 892 (1986).
[33] A. Janotti, S. B. Zhang, S.-H. Wei, and C. G. Van de Walle, Phys. Rev. Lett. **89**, 086403 (2002).
[34] J. F. Geisz, D. J. Friedman, J. M. Olson, S. R. Kurtz, and B. M. Keyes, J. Cryst. Growth **195**, 401 (1998).
[35] J. Li and S.-H. Wei, Phys. Rev. B **73**, 041201(R) (2006).
[36] W. Shan, W. Walukiewicz, J. W. Ager, E. E. Haller, J. F. Geisz, D. J. Friedman, J. M. Olson, and S. R. Kurtz, Phys. Rev. Lett. **82**, 1221 (1999).
[37] T. Mattila, S.-H. Wei, and A. Zunger, Phys. Rev. B **60**, R11245 (1999).
[38] J. D. Perkins, A. Mascarenhas, Y. Zhang, J. F. Geisz, D. J. Friedman, J. M. Olson, and S. R. Kurtz, Phys. Rev. Lett. **82**, 3312 (1999).
[39] D. J. Wolford, J. A. Bradley, K. Fry, and J. Thompson, in *Proceedings of the 17th International Conference on the Physics of Semiconductors*, edited by J. D. Chadi and W. A. Harrison (Springer, New York, 1984), p. 627.
[40] P. R. C. Kent and A. Zunger, Phys. Rev. B **64**, 115208 (2001).
[41] S.-H. Wei and A. Zunger, Appl. Phys. Lett. **72**, 2011 (1998).